ChemComm

COMMUNICATION

View Article Online
View Journal | View Issue

Cite this: *Chem. Commun.*, 2020, **56**, 11046

Received 5th June 2020,
Accepted 5th August 2020

DOI: 10.1039/d0cc03962d

rsc.li/chemcomm

Two-component supramolecular hydrogel for controlled drug release†

Anna K. Patterson and David K. Smith *

A hybrid gel has been developed by combining two supramolecular gelators. Each gelator endows the hybrid gel with its own characteristics. One gelator enables pH-mediated controlled release of the active pharmaceutical ingredient naproxen, while the other new gelator enhances mechanical stability. Self-assembly thus gives multi-functional gels with potential applications.

Supramolecular hydrogels, soft materials typically comprising *ca.* 99% water immobilised by a network of entangled fibres, are of increasing interest in biomedical applications.[1] The fibres self-assemble into a 'solid-like' network from a low-molecular-weight gelator (LMWG).[2] Self-assembled hydrogels have many attractive properties, particularly their responsive nature and generally high biocompatibility.[3] There is also the potential to program desired functionality into the bulk gel, through simple molecular-scale modifications of the LMWG.[4] This has led to increasing interest in their use in biomedical settings, including drug delivery.[5] However, supramolecular gels often have low mechanical strength, making them difficult to manipulate.

One way of enhancing the mechanical strength of supramolecular hydrogels is to combine them with polymer gelators, which are generally more mechanically robust, albeit less responsive to external stimuli.[6] Increasingly, hybrid gels comprising two or more supramolecular gelators are also being studied, with the hope that the properties of the overall gel can be modified by tuning the ratio of the components, although applications of this approach remain rare.[7] Combining multiple gelators is potentially a simple way of accessing gels with different properties.[8] When two LMWGs are combined, self-assembly can occur in different ways giving different types of self-organised material. The individual gelators may preferentially interact with other gelators of the same type, leading to 'self-sorted' fibres.[9] Alternatively, each gelator may preferentially interact with the other gelator, and fibrils will assemble with alternating gelators.[10] If the gelators have no strong preference for either interaction, then random mixing can occur.[11] Finally, one gelator may disrupt the assembly of the other through non-productive interactions, causing loss of gelation. Self-sorting gelators are desirable because orthogonal networks can be exploited to control the properties of the gel (Fig. 1).[12]

In recent years, we have investigated hydrogels based on the industrially-relevant 1,3:2,4-dibenzylidenesorbitol (DBS) framework.[13] The parent molecule (DBS) and simple derivatives, have long been exploited for thickening properties, but were not previously capable of forming hydrogels as they are too insoluble in water. By modifying the aromatic 'wings' of DBS, we developed hydrogelators.[14] One of these is **DBS-CONHNH$_2$**, with hydrophilic acyl hydrazide groups.[15] It forms a hydrogel using a simple heat/cool cycle, and is stable across a range of pH values. Hydrogels formed from **DBS-CONHNH$_2$** have been used for environmental remediation,[15] drug delivery,[16] and cell culture.[17] Controlled release of active pharmaceutical ingredients (APIs) like naproxen (NPX) can be achieved as a result of interactions between the **DBS-CONHNH$_2$** fibres and the API carboxylic acid. However, the gels are mechanically weak and difficult to manipulate. We have previously combined **DBS-CONHNH$_2$** with polymer gelators to

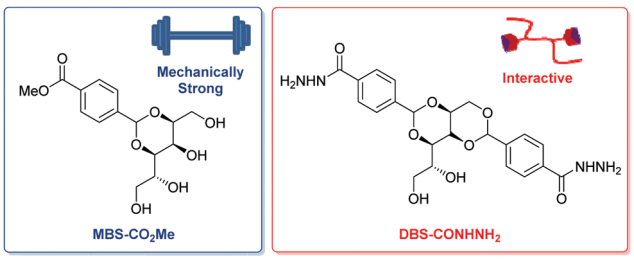

Fig. 1 The structures of hydrogelators **DBS-CONHNH$_2$** and **MBS-CO$_2$Me** investigated in this paper.

Department of Chemistry, University of York, Heslington, York, YO10 5DD, UK. E-mail: david.smith@york.ac.uk

† Electronic supplementary information (ESI) available: Materials and methods, characterisation and assay data. See DOI: 10.1039/d0cc03962d

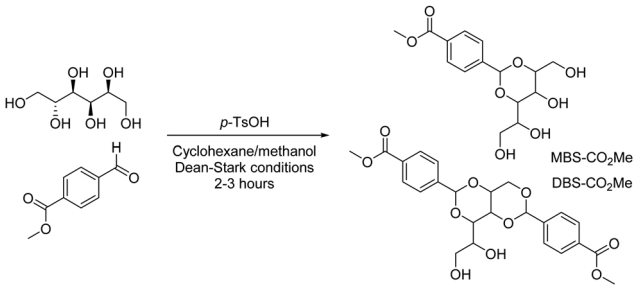

Scheme 1 The reaction of D-sorbitol and 4-methylcarboxaldehyde to give **MBS-CO_2Me** and **DBS-CO_2Me**.

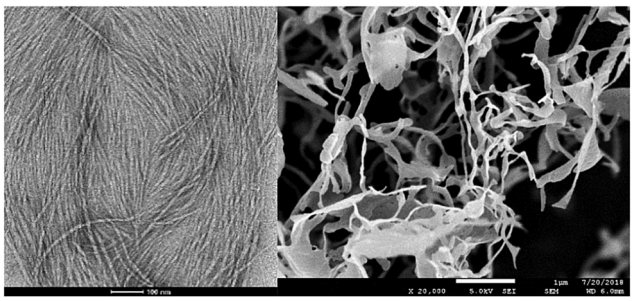

Fig. 2 Left: TEM image of an **MBS-CO_2Me** hydrogel; scale bar 100 nm. Right: SEM image of an **MBS-CO_2Me** hydrogel; scale bar 1 μm.

enhance rheological performance.[18] Here, we wanted to combine **DBS-$CONHNH_2$** with a LMWG to produce a new tuneable, responsive gel.

In the hunt for suitable LMWGs to combine with **DBS-$CONHNH_2$**, we decided to develop a new gelator, having noticed interesting properties of a by-product from its synthesis (Scheme 1). **DBS-CO_2Me** is made by condensation of D-sorbitol and 4-methylcarboxy benzaldehyde, giving mono-, di- and tri-substituted sorbitol derivatives (MBS, DBS and TBS derivatives). This reaction can be optimised for either DBS (2 : 1 aldehyde : sorbitol) or MBS product (1 : 4 aldehyde : sorbitol) (for full method and characterisation see ESI,† Fig. S1 and S2). We noticed **MBS-CO_2Me** formed effective gels in water. The ability of simpler MBS derivatives to form hydrogels is known in the literature.[19] **DBS-CO_2Me** does not form hydrogels because it is insufficiently soluble, but for **MBS-CO_2Me**, the lack of one aromatic ring, and the presence of two additional OH groups increases hydrophilicity, making it sufficiently water-soluble. The effect of solubility on gelation is increasingly understood.[20]

We investigated the properties of this new hydrogelator. Gelation was achieved *via* a heat/cool cycle, giving transparent gels (Fig. S4, ESI†). The minimum gelation concentration (MGC) was 0.75% wt/vol, with lower loadings giving solutions. SEM and TEM indicated a fibrous network. TEM shows relatively homogeneous helical fibres, with a diameter of *ca.* 8 nm (Fig. 2, left). Drying gels can cause morphological change[21] – in an attempt to limit this, we cryo-dried samples for SEM. The small nanofibres and relative lack of aggregation are consistent with the observation that gels formed by **MBS-CO_2Me** in water are transparent. This is similar to gels formed by **DBS-$CONHNH_2$**, which also have nanofibres *ca.* 10 nm in diameter.[15]

Rheology was carried out to explore the mechanical properties of the **MBS-CO_2Me** hydrogel. At a loading of 0.85% wt/vol, $G' > G''$ in the linear viscoelastic region (LVR), with G' being *ca.* 2800 Pa (Fig. S6a, ESI†). This is a significantly stiffer gel than that formed by **DBS-$CONHNH_2$** (G' = 1200 Pa). The two gels had similar elasticity, with G'/G'' crossover points of *ca.* 12%. Interestingly, **MBS-CO_2Me** was much more robust and easier to physically manipulate than **DBS-$CONHNH_2$**, with gel discs being easily transferred for rheology, with no breakage.

Variable temperature (VT) circular dichroism (CD) spectroscopy of **MBS-CO_2Me** had a maximum ellipticity at *ca.* 280 nm, showing the aromatic ring of **MBS-CO_2Me** experiences a chiral environment (Fig. S10, ESI†). This CD band was temperature-dependent, proving the chiral environment is generated by self-assembly. The most significant change in ellipticity was at 45–55 °C, supportive of a gel–sol transition at this temperature.

Simple tube inversion methodology confirmed **MBS-CO_2Me** hydrogels indeed had T_{gel} values at *ca.* 55 °C, significantly lower than **DBS-$CONHNH_2$** (*ca.* 80 °C), despite the higher concentration (Table S1, ESI†). We reason the greater hydrophilicity of **MBS-CO_2Me** makes it more temperature-sensitive, *i.e.*, it dissolves more easily on heating. When the resulting hot solutions were left to stand overnight, gels re-formed. However, rather than being transparent, they were white, with some precipitate, indicative of greater aggregation and less controlled assembly. When T_{gel} values for these re-formed gels were determined, those at lower concentrations had lower T_{gel} values, while there was little impact on the T_{gel} values at higher concentrations. These gels at higher loadings also re-formed opaque gels for a second time. Rheology indicated a slight increase in G' values.

MBS-CO_2Me gels were then tested for their ability to encapsulate and release the API naproxen (NPX, Fig. 3). This was achieved by mixing the API and gelator as solids in advance of the heat/cool cycle. Hydrogels were still formed (Table S2 and Fig. S8, ESI†), but when API release was investigated, the **MBS-CO_2Me** hydrogel broke-down rapidly (within 3 h) once the supernatant was placed on top of the gel (Fig. 3). This occurred in the presence of any supernatant, including water and a range of buffers. This was not observed with **DBS-$CONHNH_2$**, and was initially surprising given the **MBS-CO_2Me** gel is more robust. We reason that the higher solubility of **MBS-CO_2Me** makes the gel less stable to the presence of excess aqueous medium.

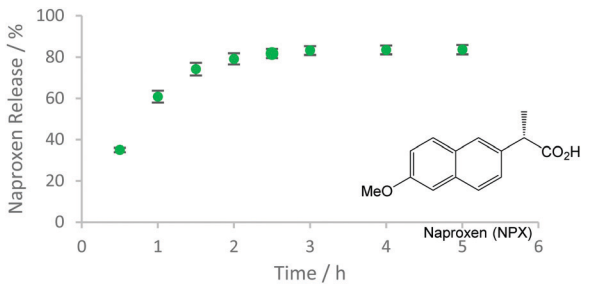

Fig. 3 Release of naproxen into pH 7 buffer from **MBS-CO_2Me** hydrogels showing rapid release driven by erosion of the gel.

NPX has a maximum absorbance at 329 nm, allowing API release to be quantified *via* UV-vis spectroscopy. When incubated at 37 °C with pH 7 buffer, around 85% of NPX was released within 3 h, roughly the point at which the gel broke down completely – we thus propose an 'erosion' mode of API release for **MBS-CO_2Me**.

We combined **MBS-CO_2Me** and **DBS-CONHNH$_2$**, hoping their different properties would be synergistic. Our goal was a hybrid gel with mechanical properties enhanced by **MBS-CO_2Me**, but maintaining the controlled release and water stability of **DBS-CONHNH$_2$**. Initially, gelation was optimised. **DBS-CONHNH$_2$** and **MBS-CO_2Me** hydrogels have very different MGCs (0.20% and 0.75% wt/vol respectively). Varying concentrations were explored, with the gelators mixed as solids. The total MGC for the hybrid gel was 0.3% wt/vol (**DBS-CONHNH$_2$** at 0.2% wt/vol, and **MBS-CO_2Me** at 0.1% wt/vol). Hybrid hydrogels formed even with both gelators below their individual MGCs (DBSCONHNH$_2$ at 0.16% wt/vol and **MBS-CO_2Me** at 0.2% wt/vol).

Hydrogels with a range of LMWG concentrations were prepared, and their thermal properties investigated. Given that **MBS-CO_2Me** hydrogels have lower T_{gel} values (*ca.* 55 °C) than **DBS-CONHNH$_2$** hydrogels (*ca.* 80 °C), it was predicted that increasing the proportion of **MBS-CO_2Me** in the hybrid gel may lower T_{gel}, providing access to a range of T_{gel} values. This was indeed the case, with T_{gel} values from 27 °C to >100 °C being obtained (Tables S3 and S4, ESI†). In general, a greater proportion of **MBS-CO_2Me** gave a lower T_{gel}, and a greater proportion of **DBS-CONHNH$_2$** gave a higher T_{gel}. Total gelator loading was also important – more gelator gave higher T_{gel} values.

SEM and TEM indicated nanofibres of *ca.* 10 nm diameter (Fig. S4 and S5, ESI†). It was not possible to differentiate nanofibres for the individual gelators, as they are similar in morphology, but it was clear self-assembly in the mixed system was not disrupted, nor did different types of assembly arise as a result of mixing.

VT ^{1}H NMR studies investigated gelator immobilisation in the hybrid gel, and understand how the LMWGs respond to an increase in temperature (Fig. 4). Hybrid gels (0.80% wt/vol **MBS-CO_2Me** and 0.22% wt/vol **DBS-CONHNH$_2$**) were prepared in an NMR tube using D_2O : H_2O (50 : 50, D_2O alone leads to reduced solubility of **MBS-CO_2Me**), with DMSO (2 μl) as an internal standard. This allows determination of the gelator assembled in the 'solid-like' network, because mobile gelator in the 'liquid-like' phase is visible in the ^{1}H NMR, and can be quantified by relative integration. At room temperature, neither gelator was observed in the spectrum, indicating both are assembled into 'solid-like' networks. As temperature increased, the signals for **MBS-CO_2Me** became visible first, from around 40 °C with around 90% being free at 65 °C. This reflects the higher solubility of **MBS-CO_2Me** and its lower T_{gel} value (see above). The signal corresponding to mobile **DBS-CONHNH$_2$** first appears at around 55 °C, and 90% of the gelator is free at 85 °C, in-line with its higher T_{gel} value. A small amount of the **DBS-CONHNH$_2$** disassembles at *ca.* 55 °C before **MBS-CO_2Me** disassembly is complete. It is therefore possible that self-sorting in this system is not perfect, but nonetheless, the networks do still largely disassemble in a sequential way and thus with a good degree of self-sorting.

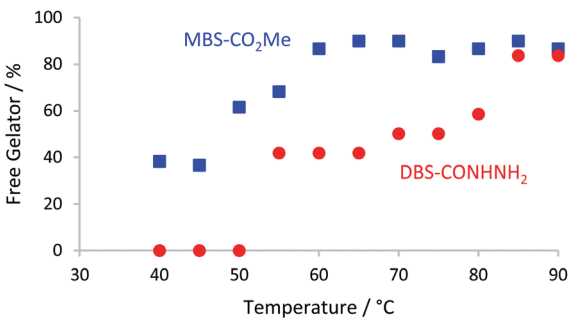

Fig. 4 The breakdown of the hybrid hydrogel on increasing temperature, with free gelator monitored by ^{1}H NMR spectroscopy. The loading of **MBS-CO_2Me** is 0.80% wt/vol, and of **DBS-CONHNH$_2$** is 0.22% wt/vol.

It was hoped the stiffer **MBS-CO_2Me** would reinforce the more interactive, but mechanically weak, **DBS-CONHNH$_2$**, giving a gel that was easier to manipulate. Hybrid hydrogels with varying loadings of **MBS-CO_2Me** ('high': 0.80% wt/vol, 'low': 0.10% wt/vol) and **DBS-CONHNH$_2$** ('high': 0.28% wt/vol, 'low': 0.24% wt/vol) were tested by rheology (Table 1 and Fig. S6, S7, ESI†). Pleasingly, with higher proportions of **MBS-CO_2Me**, the hybrid gel was stiffer than either **DBS-CONHNH$_2$** or **MBS-CO_2Me** alone (G' = 9600 Pa). At higher **MBS-CO_2Me** concentrations, increased loading of **DBS-CONHNH$_2$** leads to a slightly weaker gel, perhaps as a result of the more extensive weaker **DBS-CONHNH$_2$** network being more dominant. However, at the lowest concentrations of **MBS-CO_2Me**, where the concentration of **MBS-CO_2Me** here is below the MGC, the gels are slightly weaker than **DBS-CONHNH$_2$** alone, suggesting a small amount of **MBS-CO_2Me** network can disrupt the **DBS-CONHNH$_2$** network. Therefore, there is scope to tune the rheological properties of the hybrid hydrogel, to give properties suitable for the desired application.

Given **DBS-CONHNH$_2$** can achieve pH-mediated naproxen release,[18] we wanted to determine if this ability was retained by the hybrid gel, and thus investigated encapsulation and release of NPX. Stable gels were still formed in the presence of NPX, and the addition did not have a significant impact on the rheological properties of the hydrogels – there was perhaps a slight stiffening reflected by a small increase in G' (Fig. S8 and S9, ESI†). We studied the interaction of the hybrid gels with NPX by ^{1}H NMR. A known mass of each gelator and NPX, were dissolved in D_2O : H_2O

Table 1 G' and G'' values, from the LVER, for **MBS-CO_2Me** (high – 0.80% wt/vol, low – 0.10% wt/vol) and **DBS-CONHNH$_2$** ('high' – 0.28% wt/vol, 'low' – 0.24% wt/vol) gels

Gelator	G'/Pa	G''/Pa
DBS-CONHNH$_2$	1200	60
MBS-CO_2Me	2800	550
High MBS, low DBS	9600	700
High MBS, high DBS	6300	900
Low MBS, low DBS	300	25
Low MBS, high DBS	500	30

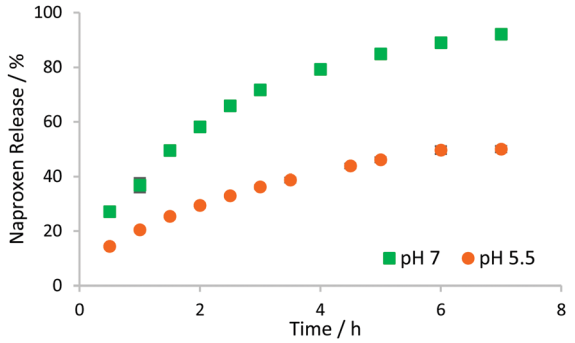

Fig. 5 Release of NPX, from hybrid hydrogels based on **DBS-CONHNH$_2$** (0.20% wt/vol) and **MBS-CO$_2$Me** (0.70% wt/vol) at varying pH values.

(50 : 50), and the hydrogel formed in an NMR tube. An internal standard (DMSO) was added to allow quantification of any 'mobile' NPX. These studies indicated that, like **DBS-CONHNH$_2$** gels, over 90% of the NPX was not visible in the NMR spectrum, and is therefore likely bound to the gel network as a result of non-covalent interactions between the acid on NPX and the hydrazide. The interactive properties of **DBS-CONHNH$_2$** thus appear to translate into the mechanically-robust hybrid gel.

The release of NPX from the hybrid gels, into buffers with different pH values, was then investigated by monitoring the UV-vis absorbance at 329 nm. Pleasingly, the supramolecular hybrid gel showed pH-dependent release (Fig. 5). The NPX release profile at pH 7 is similar to that observed previously for **DBS-CONHNH$_2$**,[16] with rapid initial release, and total release of 85–95%. In contrast, release at pH 5.5 is slower and much less favoured, reaching only *ca.* 35% in the first 3 h, and a maximum of just 55%. This is a result of the interactions between **DBS-CONHNH$_2$** fibres and NPX, which occur when NPX is protonated. The pK_a of NPX is 4.15,[22] and at pH 5.5 a greater proportion of NPX will be protonated than at higher pH values, and thus able to interact with gel nanofibres, limiting release. This controlled release is very different to the erosion release observed when using **MBS-CO$_2$Me** alone, and is attractive for oral delivery. It has the potential to reduce uptake in the acidic stomach, facilitating drug protection, and may assist controlled release in the small intestine. This is important for NSAIDs such as NPX, which have known side effects in the upper gastrointestinal tract[23] Changing LMWG concentrations had little effect on the release process (Fig. S11 and S12, ESI†).

In summary, a two-component supramolecular hydrogel, formed from two gelators (**DBS-CONHNH$_2$** and novel MBS-CO$_2$M), has been used to encapsulate and release NPX. NMR studies indicate that the gel has sequentially assembled networks. Each gelator has its own unique characteristics programmed into the performance of the gel. Specifically, the hybrid gel retains the interactive nature of **DBS-CONHNH$_2$**, facilitating controlled drug release, while having improved mechanical strength as a result of **MBS-CO$_2$Me**. NPX release is pH-mediated, lower pH leading to less release, with potential for controlled release in the small intestine. Further work will focus on tuning multi-component hydrogels to give different release profiles, enabling other drug delivery applications, as well as investigating such gels in wider biomedical applications like tissue engineering or wound healing.

Conflicts of interest

There are no conflicts to declare.

Notes and references

1 (*a*) B. Hu, C. Owh, P. L. Chee, W. R. Leow, X. Liu, Y.-L. Wu, P. Guo, X. J. Loh and X. Chen, *Chem. Soc. Rev.*, 2018, **47**, 6917–6929; (*b*) L. Saunders and P. X. Ma, *Macromol. Biosci.*, 2019, **19**, 1800313.
2 (*a*) R. G. Weiss, *J. Am. Chem. Soc.*, 2014, **136**, 7519–7530; (*b*) E. R. Draper and D. J. Adams, *Chem*, 2017, **3**, 390–410.
3 X. Du, J. Zhou, J. Shi and B. Xu, *Chem. Rev.*, 2015, **115**, 13165–13307.
4 *Molecular Gels: Structure and Dynamics*, ed. R. G. Weiss, Royal Society of Chemistry, Cambridge, 2018.
5 (*a*) K. J. Skilling, F. Citossi, T. D. Bradshaw, M. Ashford, B. Kellam and M. Marlow, *Soft Matter*, 2014, **10**, 237–256; (*b*) A. Vashist, A. Kaushik, K. Alexis, R. D. Jayant, V. Sagar, A. Vashist and M. Nair, *Curr. Pharm. Des.*, 2017, **23**, 3595–3602; (*c*) J. Mayr, C. Saldías and D. Díaz Díaz, *Chem. Soc. Rev.*, 2018, **47**, 1484–1515.
6 D. J. Cornwell and D. K. Smith, *Mater. Horiz.*, 2015, **2**, 279–293.
7 (*a*) L. E. Buerkle and S. J. Rowan, *Chem. Soc. Rev.*, 2012, **41**, 6089–6102; (*b*) J. Raeburn and D. J. Adams, *Chem. Commun.*, 2015, **51**, 5170–5180.
8 E. R. Draper and D. J. Adams, *Chem. Soc. Rev.*, 2018, **47**, 3395–3405.
9 (*a*) J. R. Moffat and D. K. Smith, *Chem. Commun.*, 2009, 316–318; (*b*) E. R. Draper, E. G. B. Eden, T. O. McDonald and D. J. Adams, *Nat. Chem.*, 2015, **7**, 848–852; (*c*) N. Singh, K. Zhang, C. A. Angulo-Pachón, E. Mendes, J. H. van Esch and B. Escuder, *Chem. Sci.*, 2016, **7**, 5568–5572; (*d*) S. Onogi, H. Shigemitsu, T. Yoshii, T. Tanida, M. Ikeda, R. Kubota and I. Hamachi, *Nat. Chem.*, 2016, **8**, 743–752; (*e*) E. R. Draper, B. Dietrich and D. J. Adams, *Chem. Commun.*, 2017, **53**, 1864–1867; (*f*) R. Kubota, S. Liu, H. Shigemitsu, K. Nakamura, W. Tanaka, M. Ikeda and I. Hamachi, *Bioconjugate Chem.*, 2018, **29**, 2058–2067; (*g*) C. C. Piras and D. K. Smith, *Chem. – Eur. J.*, 2019, **25**, 11318–11326; (*h*) B. O. Okesola, Y. Wu, B. Derkus, S. Gani, D. Wu, D. Knani, D. K. Smith, D. J. Adams and A. Mata, *Chem. Mater.*, 2019, **31**, 7883–7897.
10 (*a*) M. Tena-Solsona, S. Alonso-de Castro, J. F. Miravet and B. Escuder, *J. Mater. Chem. B*, 2014, **2**, 6192–6197; (*b*) G.-F. Liu, W. Ji, W.-L. Wang and C.-L. Feng, *ACS Appl. Mater. Interfaces*, 2015, **7**, 301–307.
11 (*a*) D. M. Ryan, T. M. Doran and B. L. Nilsson, *Chem. Commun.*, 2011, **47**, 475–477; (*b*) H. A. M. Ardoña, E. R. Draper, F. Citossi, M. Wallace, L. C. Serpell, D. J. Adams and J. D. Tovar, *J. Am. Chem. Soc.*, 2017, **25**, 8685–8692.
12 C. Colquhoun, E. R. Draper, E. G. B. Eden, B. N. Cattoz, K. L. Morris, L. Chen, T. O. McDonald, A. E. Terry, P. C. Griffiths, L. C. Serpell and D. J. Adams, *Nanoscale*, 2014, **6**, 13719–13725.
13 B. O. Okesola, V. M. P. Vieira, D. J. Cornwell, N. K. Whitelaw and D. K. Smith, *Soft Matter*, 2015, **11**, 4768–4787.
14 D. K. Smith, *Chem. Commun.*, 2018, **54**, 4743–4760.
15 B. O. Okesola and D. K. Smith, *Chem. Commun.*, 2013, **49**, 11164–11166.
16 E. J. Howe, B. O. Okesola and D. K. Smith, *Chem. Commun.*, 2015, **51**, 7451–7454.
17 V. M. P. Vieira, A. C. Lima, M. de Jong and D. K. Smith, *Chem. – Eur. J.*, 2018, **24**, 15112–15118.
18 (*a*) P. R. A. Chivers and D. K. Smith, *Chem. Sci.*, 2017, **8**, 7218–7227; (*b*) C. C. Piras, P. Slavik and D. K. Smith, *Angew. Chem., Int. Ed.*, 2020, **59**, 853–859; (*c*) P. R. A. Chivers, J. A. Kelly, M. J. S. Hill and D. K. Smith, *React. Chem. Eng.*, 2020, **5**, 1112–1117.
19 (*a*) J. Song, H. Sun, S. Sun and R. Feng, *Trans. Tianjin Univ.*, 2013, **19**, 319–325; (*b*) K. Fan, H. Kong, X. Yang and J. Song, *RSC Adv.*, 2016, **6**, 80934–80938; (*c*) G. C. Dizon, G. Atkinson, S. P. Argent, L. T. Santu and D. B. Amabilino, *Soft Matter*, 2020, **16**, 4640–4654.
20 Y. Lan, M. G. Corradini, R. G. Weiss, S. R. Raghavan and M. A. Rogers, *Chem. Soc. Rev.*, 2015, **44**, 6035–6058.
21 D. J. Adams, *Gels*, 2018, **4**, 32–37.
22 F. Barbato, M. I. La Rotonda and F. Quaglia, *J. Pharm. Sci.*, 1997, **86**, 225–229.
23 N. Bhala and J. Emberson, *et al.*, *Lancet*, 2013, **382**, 769–779.